Schizophrenia Research 182 (2017) 74–83

Contents lists available at ScienceDirect

Schizophrenia Research

journal homepage: www.elsevier.com/locate/schres

Novel gene-brain structure relationships in psychotic disorder revealed using parallel independent component analyses

Neeraj Tandon , BS [a,b,*], Pranav Nanda, MS [a,c], Jaya L. Padmanabhan, MD [a], Ian T. Mathew, BA [a], Shaun M. Eack, PhD [d], Balaji Narayanan, PhD [e,f], Shashwath A. Meda, MS [e,f], Sarah E. Bergen, PhD [g,h,i], Gualbert Ruaño, MD, PhD [j], Andreas Windemuth, PhD [j], Mohan Kocherla, MS [j], Tracey L. Petryshen, PhD [g,h], Brett Clementz, PhD [k], John Sweeney, PhD [l], Carol Tamminga, MD [l], Godfrey Pearlson, MD [e,f], Matcheri S. Keshavan, MD [a]

[a] Psychiatry, Harvard Medical School, Beth Israel Deaconess Medical Ctr, Boston, MA, USA
[b] Baylor College of Medicine, Texas Medical Center, Houston, TX, USA
[c] College of Physicians & Surgeons, Columbia University Medical Center, New York, NY, USA
[d] School of Social Work, University of Pittsburgh, Pittsburgh, PA, USA
[e] Olin Neuropsychiatry Research Center, Hartford, CT, USA
[f] Department of Psychiatry and Neurobiology, Yale University, New Haven, CT, USA
[g] Psychiatric and Neurodevelopmental Genetics Unit, Center for Human Genetic Research and Department of Psychiatry, Massachusetts General Hospital, Boston, MA, USA
[h] Stanley Center for Psychiatric Research, Broad Institute of Harvard and MIT, Cambridge, MA, USA
[i] Medical Epidemiology and Biostatistics, Karolinska Institute, Stockholm, Sweden
[j] Genomas, Inc, Hartford, CT, USA
[k] Department of Psychology, Department of Neuroscience, Bio-Imaging Research Center, University of Georgia, Athens, GA, USA
[l] Psychiatry, UT Southwestern, Dallas, TX, USA

ARTICLE INFO

Article history:
Received 29 June 2016
Received in revised form 14 October 2016
Accepted 16 October 2016
Available online 24 October 2016

Keywords:
Genes
Brain structure
MRI
Intermediate phenotype
Schizophrenia
Bipolar disorder
Schizoaffective disorder
Endophenotype
Nosology

ABSTRACT

Background: Schizophrenia, schizoaffective disorder, and psychotic bipolar disorder overlap with regard to symptoms, structural and functional brain abnormalities, and genetic risk factors. Neurobiological pathways connecting genes to clinical phenotypes across the spectrum from schizophrenia to psychotic bipolar disorder remain largely unknown.
Methods: We examined the relationship between structural brain changes and risk alleles across the psychosis spectrum in the multi-site Bipolar-Schizophrenia Network for Intermediate Phenotypes (B-SNIP) cohort. Regional MRI brain volumes were examined in 389 subjects with a psychotic disorder (139 schizophrenia, 90 schizoaffective disorder, and 160 psychotic bipolar disorder) and 123 healthy controls. 451,701 single-nucleotide polymorphisms were screened and processed using parallel independent component analysis (para-ICA) to assess associations between genes and structural brain abnormalities in probands.
Results: 482 subjects were included after quality control (364 individuals with psychotic disorder and 118 healthy controls). Para-ICA identified four genetic components including several risk genes already known to contribute to schizophrenia and bipolar disorder and revealed three structural components that showed overlapping relationships with the disease risk genes across the three psychotic disorders. Functional ontologies representing these gene clusters included physiological pathways involved in brain development, synaptic transmission, and ion channel activity.
Conclusions: Heritable brain structural findings such as reduced cortical thickness and surface area in probands across the psychosis spectrum were associated with somewhat distinct genes related to putative disease pathways implicated in psychotic disorders. This suggests that brain structural alterations might represent discrete psychosis intermediate phenotypes along common neurobiological pathways underlying disease expression across the psychosis spectrum.

© 2016 Elsevier B.V. All rights reserved.

1. Introduction

The etiopathology of psychotic disorders ranging from schizophrenia (SZ) through schizoaffective disorder (SAD) to psychotic bipolar

* Corresponding author at: Beth Israel Deaconess Medical Center and Massachusetts Mental Health Center, 75 Fenwood Rd, STE 549, Boston, MA 02115, USA.
E-mail address: ntandon@bidmc.harvard.edu (N. Tandon).

http://dx.doi.org/10.1016/j.schres.2016.10.026
0920-9964/© 2016 Elsevier B.V. All rights reserved.

disorder (PBP) is being increasingly clarified with the identification of specific putative genes and the characterization of a range of structural and functional brain abnormalities (Keshavan et al., 2008; PGC Consortium et al., 2014; Tandon et al., 2008). Large-scale genomic studies, including genome-wide association studies, have begun to implicate a number of common as well as unique loci and polymorphisms in SZ and PBP (Gatt et al., 2015). Several gene variants that underlie brain development, immune mechanisms, synaptic function and ion channels have been identified (Gratten et al., 2014). Structural brain abnormalities in SZ include gray matter volume reductions in several brain regions notably frontal and temporal cortex and subcortical regions such as hippocampus, thalamus and basal ganglia (Keshavan et al., 2008). Despite delineation of a range of neurobiological findings in patients with these conditions (Ellison-Wright et al., 2010; McDonald et al., 2006; Palaniyappan et al., 2012), their functional characterization is poorly defined and the specific pathways from etiology through pathology to clinical expression remain largely unidentified (Keshavan et al., 2011a, b).

Investigation of disease risk-related, heritable phenotypes (i.e. endophenotypes) such as neuroanatomical alterations can serve as a foot-hold in discerning the neurobiological pathways connecting genes to clinical phenotypes across the psychosis spectrum (Gottesman and Gould, 2003; Glahn, et al., 2014; Insel and Cuthbert, 2009). Structural brain abnormalities in psychotic disorders include gray matter volume reductions in several brain regions notably the frontal and temporal cortex and subcortical regions such as the hippocampus, thalamus and basal ganglia, and may serve as potential endophenotypes (Keshavan et al., 2008). However, a significant barrier to an improved understanding of the nature of various psychotic disorders is our current symptom-based nosological system which does not reliably separate biologically distinct categories and thus "does not carve nature at its joints" (Kapur et al., 2012). Although SZ, SAD, and PBP have been considered distinct clinical entities for almost a century (Kraepelin, 1919; Tandon R, 2008), there are several overlaps in disease risk genes, structural and functional intermediate phenotypes, and symptomatology and the boundaries between these diagnoses have increasingly been called into question (Hyman, 2010).

A dimensional approach examining neurobiological alterations and their genetic underpinnings agnostic to diagnosis is more likely to identify valid disease processes across the spectrum of psychotic disorders (Keshavan et al., 2011a, b). The Bipolar-Schizophrenia Network on Intermediate Phenotypes (B-SNIP) is a multi-site research collaboration established to delineate pathophysiological pathways in psychotic disorders. It focuses on examining the manifestation and distribution of a range of informative endophenotypes across the psychosis spectrum (spanning SZ, SAD, and PBP) and evaluating their genetic associations (Hill et al., 2013; Ivleva et al., 2013; Tamminga et al., 2013).

Challenges posed by limitations to processing multidimensional data are inherent in the endeavor to define pathways across domains. Specifically, discovery of multiple genes contributing to these molecular biological processes is a challenge with traditional univariate methods. In order to evaluate relationships between interacting disease risk genes and structural brain findings across psychotic disorders, one can utilize novel multivariate data-driven statistical techniques that allow simultaneous analysis of multiple modalities. One such approach is parallel independent component analysis (para-ICA) (Chen et al., 2012; Liu et al., 2008; Sui et al., 2011). Unlike univariate studies such as GWAS, para-ICA identifies linearly interacting risk gene variants, which taken together contribute to a quantitative trait, and when taken together may elucidate illness-associated molecular/biological pathways (Meda et al., 2014; Pearlson et al., 2015). The selection of a proper endophenotype is also critical, and a chief assumption in the selection of the endophenotype is that its biological pathways will be relatively closer to the action of the genes (Gottesman and Gould, 2003; Insel and Cuthbert, 2009). We addressed this by using cortical thickness and cortical surface area, measures demonstrated to be independently heritable of each other and likely to be more proximal to genetic action compared to volumetric measures commonly used in previous studies (Panizzon et al., 2009).

In this study, we applied this approach to investigate gene-brain structure relationships in patients with schizophrenia, schizoaffective disorder, and psychotic bipolar disorder. Beginning with genetic and structural brain data (single nucleotide polymorphisms [SNPs] and MRI-derived regional brain measures, respectively), we employed para-ICA to uncover underlying factors from both modalities and their relationships across psychotic disorders. We aimed to examine the association between structural components and risk genes across the psychosis spectrum (agnostic to categorical DSM diagnosis) from probands with SZ, SAD, PBP, and in healthy controls all enrolled in B-SNIP in order to determine their candidacy as potential intermediate/endophenotypes in biologically interactive disease pathways. We hypothesized that: a) we would observe structural differences such as altered cortical thickness and surface area in psychosis probands versus healthy controls, and b) that such alterations would be differentially associated with sets of genes that govern synaptic function, brain development, neuronal ion channels, and inflammatory processes previously known to be associated with psychosis risk.

2. Materials and methods

2.1. Study participants

Data were derived from the B-SNIP database on 512 subjects: 389 subjects with a psychotic disorder (139 schizophrenias, 90 schizoaffective disorders, and 160 psychotic bipolar disorders) and 123 healthy controls; 248 males, 264 females. These data included 3.0 Tesla structural MRI scans, Illumina SNP genotyping data (http://www.illumina.com; Li et al., 2008a, b, and clinical/demographic information. The institutional review boards at each of the six B-SNIP sites (Chicago, Hartford, Dallas, Detroit, Maryland and Boston) approved the study and all participants provided written informed consent. Inclusion criteria for subjects were based on a diagnosis of schizophrenia, schizoaffective disorder, psychotic bipolar disorder, or healthy controls confirmed by the Structured Clinical Interview for DSM-IV Disorders (Endris et al., 2002; First et al., 2002).

2.2. Single nucleotide polymorphism (SNP) genotype data collection and preprocessing

For all subjects for whom genotyping and morphometric data were available (N = 512), we extracted DNA from a blood sample and processed single nucleotide polymorphisms (SNPs) on an Illumina Infinium HumanOmni1-Quad microarray assay (http://www.illumina.com) covering 1,140,419 SNP loci at Genomas (Hartford, CT).

SNP genotype data underwent two pre-processing stages. We first applied a series of standard quality control measures developed to remove DNA samples and markers that might introduce bias in case-control studies (Anderson et al., 2010). Genotype data were preprocessed in PLINK (Purcell et al., 2007) following a published workflow reported by Anderson et al. (2010), combining both per-individual and per-marker quality control (see Supplementary Fig. 1). In this manner, we excluded individuals with discordant gender information, elevated missing data rates, outlying heterozygosity rates, and those who were duplicated or related. We applied thresholds for minor allele frequency of 1% and a Hardy-Weinberg equilibrium p value of 0.00001. 451,701 SNPs for 482 subjects passed quality control and were carried over to the next processing stage. SNPs in high linkage disequilibrium (LD) were first removed (window 50 SNPs, $r^2 > 0.5$) to increase independence between markers. Genotype data were then subjected to a principal component analysis (PCA) using custom Matlab scripts (Mathworks, Natick, MA) to identify stratifying factors using an algorithm similar to EIGENSTRAT (Price et al., 2006). Data were adjusted

using the top three eigenvectors to exclude any underlying stratification and SNPs then were statistically prioritized for para-ICA using logistic regression between the proband group and controls in a disease-association analysis. All SNPs significantly associated with any of the three diseases at a nominal $p < 0.05$ uncorrected threshold were retained for further analysis, achieving the important goals of 1) effectively restricting core analyses to potentially disease-related genetic data in the current sample, and 2) reducing potential noise from other interacting genes with minimal relationship to the disease model, thereby providing data-driven "enhancement" (Dawy et al., 2008). After genetic-quality control and preprocessing, 482 total subjects and 12,207 SNPs remained for the final para-ICA analysis. Supplementary Fig. 1 illustrates the general processing workflow.

2.3. MRI-structural imaging phenotype

We extracted 154 regional MRI brain measures from the 482 post-QC subjects (364 individuals with psychotic disorder and 118 healthy controls) using FreeSurfer version 5.1 (Arnold et al., 2015; Desikan et al., 2006). High-resolution isotropic T1-weighted MPRAGE sequences were obtained following the Alzheimer's Disease Neuroimaging Initiative (ADNI) protocol (Jack et al., 2008) and the images were processed by experienced analysts. Cortical thickness, surface area and volume measures were obtained using methods described previously (Arnold et al., 2015). Values were normalized by Z-score transformation, and residualized for age, sex and site covariates before they were entered into para-ICA.

2.4. Genotype-phenotype associations (para-ICA)

Parallel ICA with the MRI and the SNP data was implemented using the Fusion ICA Toolbox v2.0c (Rachakonda et al., 2008) in Matlab (Mathworks, Natick, MA) to compute independent genetic/imaging networks and simultaneously identify and quantify association between these two modalities. This variant of ICA is designed for multimodal processing and enhances the interconnection by maximizing the linkage function in a joint estimation process (Calhoun et al., 2009). It has been usefully applied to reveal gene-structure pathways in other disorders with modest sample sizes (Meda et al., 2012). Loading parameters were estimated for the weight of each component and overall correlation values between loading coefficients of the two sets of imaging and genetic components were calculated for the sample to identify significantly associated feature sets. The process for para-ICA is described in our previously published work (Chen et al., 2012; Meda et al., 2014) and in Supplementary Fig. 2. The number of independent estimated components for both SNP (dbSNP) and imaging data (6) were separately estimated using Akaike information criteria (Calhoun et al., 2001). 1000 permutations of the para-ICA were run to establish a test statistic distribution for p-values. Components were tested for internal stability by using a leave-one-out approach.

Correlation values between parallel ICA sets were appropriately corrected for multiple comparisons using a Bonferroni correction based on 60 comparisons (10 SNPs and 6 anatomical components), yielding a corrected p value threshold of 0.0008. Once significant feature set associations were identified, all contributing SNPs/imaging ROIs across each associated component were thresholded at a supra level $[Z] > 2.0$ to specifically identify dominant loadings for each individual network (Calhoun et al., 2009).

Significant SNPs from each component were batch queried against the dbSNP database (dbSNP, Bethesda, MD) to extract known gene information. The genes were subsequently entered component-wise into the MetaCore annotation software GeneGo (Thompson Reuters, New York, NY) to determine enriched biological pathways associated with structural abnormalities. Enrichment and visualization of significant SNPs mapped onto their respective genes were carried out to interpret results in the context of a curated biological knowledge base. Functional enrichment was derived in multiple ontologies, including pathways, network processes, diseases, gene ontology processes, and metabolic networks. Quantitative enrichment scores were calculated using a hyper-geometric approach to estimate the likelihood that significant genes were overrepresented in particular biological pathways, networks, or processes. Significance values were adjusted using false discovery rate (FDR) correction for multiple comparisons.

3. Results

The age (mean/standard deviation) and gender (male/female) distribution of healthy controls and subjects with a psychotic disorder were 37.4/12.3 years, 51 male/67 female and 35.8/12.5 years and 180 male/184 female respectively. There were no significant differences in age or gender distribution between healthy controls and probands with a psychotic disorder or between the three psychotic disorder groups.

3.1. Structural brain differences and heritability

All three proband groups showed significant differences from healthy controls in the global cortical thickness, cortical surface area, and subcortical volume measures (see Fig. 1). The structural brain measures evaluated were also all highly heritable ($h^2r > 0.6$) within families of probands (see Supplementary Table 1).

3.2. Parallel ICA results

Four significant associations were identified, 4 of the 10 genetic/SNP components were significantly correlated to 3 of the 6 anatomic components (represented as yellow, blue and red components respectively in Fig. 2); these associations were significant after Bonferroni correction ($p < 0.0008$). Significant differences were found in loading coefficients between healthy controls and probands for all significantly correlated

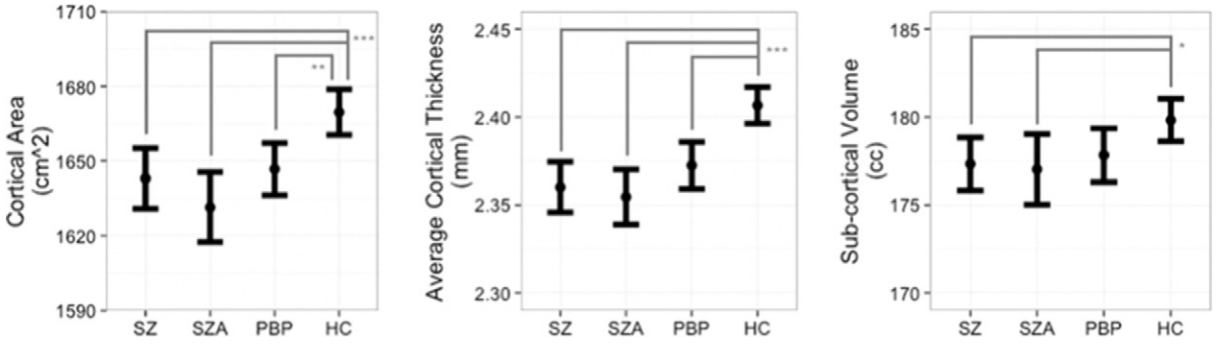

Fig. 1. The three kinds of cortical measures examined all demonstrated differences between probands and healthy controls after controlling for ICV (in the case of area and volume) and multiple comparisons.

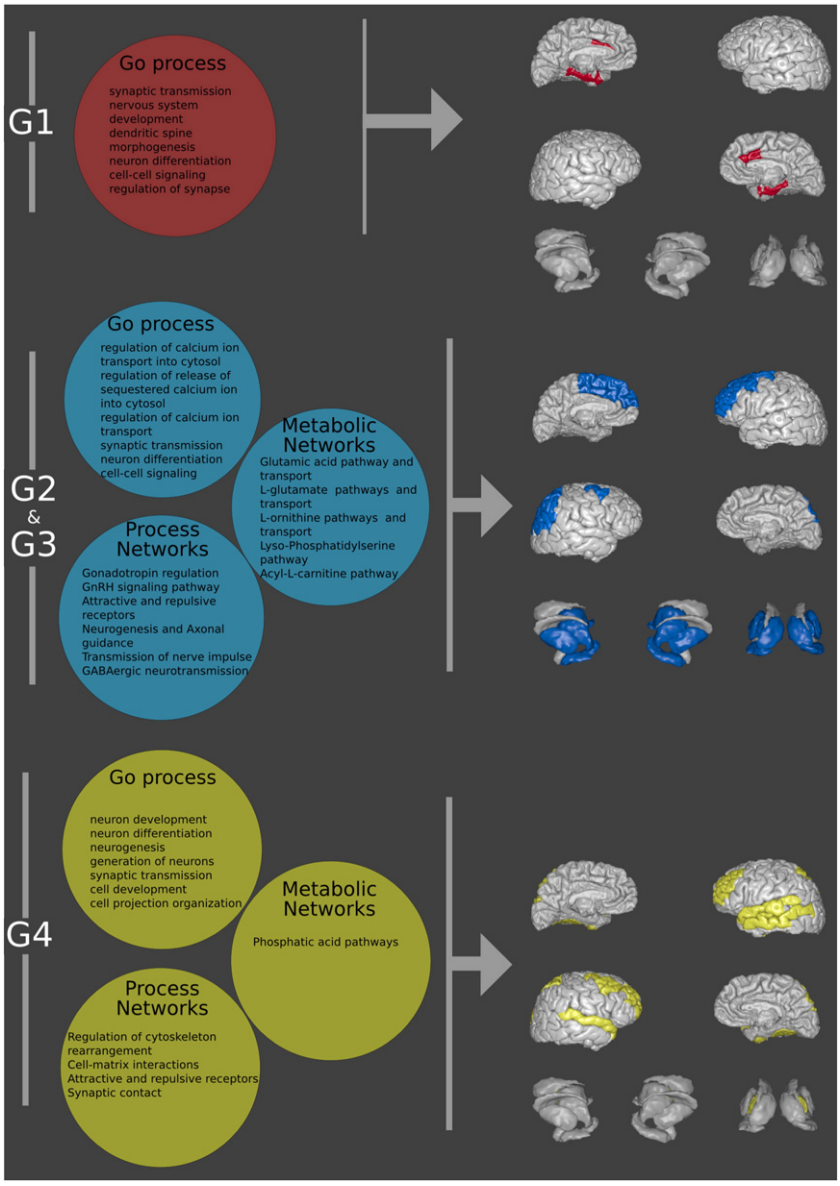

Fig. 2. Legend - RED (S1-G1): left caudal anterior cingulate thickness, left entorhinal thickness, left parahippocampal thickness, right caudal anterior cingulate thickness, right entorhinal thickness, right parahippocampal thickness; blue (S2-G2/G3): left thalamus volume, left putamen volume, left hippocampus volume, right thalamus volume, right putamen volume, right hippocampus volume, left caudal middle frontal thickness, left superior frontal thickness, left rostral middle frontal thickness, right inferior parietal thickness, right caudal middle frontal thickness, right superior parietal thickness; yellow (s3-g4): left fusiform surface area, left superior temporal surface area, left middle temporal surface area, left superior parietal surface area, left rostral middle frontal surface area, right fusiform surface area, right superior temporal, right rostral middle frontal, right superior parietal, right caudal middle frontal, right superior parietal surface area, left pallidum volume, right pallidum volume.

structural and SNP components. Structural component S2 (blue), comprised decreased thickness in the bilateral prefrontal and right parietal cortices, and volume of bilateral subcortical regions (globus pallidum, putamen, and hippocampus bilaterally), was positively correlated with genetic components G2 ($r = 0.365$; $p < 0.0001$) and with G3 ($r = -0.314$; $p < 0.0001$). Decreased loading on G2 and increased loading on G3 was related to decreased surface area and pallidal volumes. Structural component S1 (red) was positively linked to a genetic component G1 ($r = 0.407$, $p < 0.0001$); decreased loading in S1 was related to decreased paralimbic (entorhinal, parahippocampal and anterior cingulate) thickness measures. Structural component S3 (yellow) negatively correlated with genetic component G4 ($r = -0.317$; $p < 0.0001$). For a full listing of structures identified with each component, see Supplementary Table 2. This indicates that increases in G4 loading were associated with alterations in surface area measures and volume of the pallidum bilaterally. The reliability of these correlations was supported by the leave-one-out testing, with a reliability value of >0.81. Among the three identified structural components, S1 and S2 specific cortical thickness measures, whereas S3 comprised of surface area measures (Fig. 2a,b,c). Additionally, S1 and S2 included subcortical volumes (Fig. 2a,c). GeneGO pathways associated with the genetic components are listed in Fig. 2 and Table 1. Among the identified structural-genetic networks, the individual SNPs most significantly associated with these genetic components are enumerated with their gene annotations in Supplementary Table 3.

4. Discussion

Salient findings of the study include identification of four genetic-structural networks that showed somewhat distinct relationships between disease risk genes and structural abnormalities across the three psychotic disorders.

Table 1
Results of enrichment analysis from MetaCore annotation software GeneGo. Biological pathways, process networks and metabolic networks are listed for each gene cluster derived from the parallel-ICA analysis.

G1 pathway maps

#	Map	p (uncorr)	p (FDR)	(Genes in data) (Genes total)
1	Immune response: Th1 and Th2 cell differentiation	0.00005	0.008	4/40
2	Immune response: naive CD4 + T cell differentiation	0.00008	0.008	4/46
3	G-protein signaling: RhoA regulation pathway	0.0007	0.03	3/34
4	Immune response: immune responses in asthma (schema)	0.0007	0.03	2/8
5	G-protein signaling: Rap1B regulation pathway	0.001	0.04	2/11
6	Immune response: CRTH2 signaling in Th2 cells	0.001	0.04	3/44
7	Cell adhesion: ephrin signaling	0.002	0.04	3/45
8	PDE4 regulation of cyto/chemokine expression in inflammatory skin diseases	0.002	0.05	3/50
9	Neurophysiological process: synaptic vesicle fusion and recycling in nerve terminals	0.002	0.05	3/52
10	Intercellular relations in asthma (general schema)	0.003	0.06	2/16

G1 process networks

#	Network	p (uncorr)	p (FDR)	(Genes in data) (Genes total)
1	Cell adhesion: synaptic contact	0.0009	0.08	7/184
2	Cell adhesion: attractive and repulsive receptors	0.004	0.13	6/175
3	Development: neurogenesis and synaptogenesis	0.004	0.13	6/180
4	Inflammation: histamine signaling	0.01	0.18	6/213
5	Development: regulation of angiogenesis	0.01	0.18	6/223
6	Development: neurogenesis and axonal guidance	0.01	0.18	6/230
7	Inflammation: IL-12,15,18 signaling	0.01	0.18	3/59
8	Cytoskeleton: cytoplasmic microtubules	0.02	0.18	4/115
9	Signal transduction: WNT signaling	0.02	0.18	5/177
10	Immune response: T helper cell differentiation	0.03	0.26	4/140

G1 metabolic networks

1	Decanoylcarnitine pathway	0.002	0.08	3/86
2	Lauroylcarnitine pathway	0.003	0.08	3/91
3	(L)-carnitine pathway	0.03	0.11	2/82
4	CYP2D6-3-Glucagon-HNF4	0.03	0.11	2/84
5	CYP2D6-5-Glucagon-HNF4	0.03	0.11	2/87
6	CYP3A4-11-Glucagon-HNF4	0.03	0.11	2/88
7	CYP2C9-1-Glucagon-HNF4alpha	0.03	0.11	2/90
8	CYP3A4-12-Glucagon-HNF4	0.03	0.11	2/91
9	CYP3A4-1-Glucagon-HNF4	0.03	0.11	2/92
10	CYP2C9-2-Glucagon-HNF4alpha	0.03	0.11	2/92

G1 GO processes

#	Process	p (uncorr)	p (FDR)	(Genes in data) (Genes total)
1	Synaptic transmission	2×10^{-8}	7×10^{-5}	22/856
2	Nervous system development	2×10^{-7}	0.0003	40/2721
3	Dendritic spine morphogenesis	7×10^{-7}	0.0006	41741
4	Neuron differentiation	1×10^{-6}	0.0006	25/1346
5	Cell-cell signaling	1×10^{-6}	0.0006	24/1268
6	Regulation of synapse organization	2×10^{-6}	0.0006	7/90
7	Cell adhesion	2×10^{-6}	0.0006	21/1015
8	Regulation of synapse assembly	2×10^{-6}	0.0006	6/58
9	Regulation of macrophage activation	2×10^{-6}	0.0006	5/33
10	Biological adhesion	2×10^{-6}	0.0006	21/1026

G2 pathway maps

#	Map	p (uncorr)	p (FDR)	(Genes in data) (Genes total)
1	Neurophysiological process: GABA-B receptor-mediated regulation of glutamate signaling in Purkinje cells	2×10^{-5}	0.007	4/27
2	Cell adhesion: ephrin signaling	0.0001	0.02	4/45
3	Transport: alpha-2 adrenergic receptor regulation of ion channels	0.0002	0.02	4/47
4	Development: mu-type opioid receptor signaling via beta-arrestin	0.0004	0.03	3/24
5	Cell adhesion: cadherin-mediated cell adhesion	0.0005	0.03	3/26
6	Reproduction: GnRH signaling	0.0009	0.05	4/72
7	Development: S1P1 receptor signaling via beta-arrestin	0.0011	0.06	3/34
8	Upregulation of MITF in melanoma	0.0013	0.06	3/36
9	Neurophysiological process: delta-type opioid receptor in the nervous system	0.0017	0.06	3/40
10	Neurophysiological process: ACM1 and ACM2 in neuronal membrane polarization	0.0017	0.06	3/40

Table 1 (*continued*)

G2 process networks

#	Network	p (uncorr)	p (FDR)	(Genes in data) (Genes total)
1	Cell adhesion: synaptic contact	1×10^{-9}	1×10^{-7}	15/184
2	Development: neurogenesis and synaptogenesis	7×10^{-8}	4×10^{-6}	13/180
3	Development: neurogenesis and axonal guidance	4×10^{-5}	0.001	11/230
4	Reproduction: gonadotropin regulation	6×10^{-5}	0.002	10/199
5	Neurophysiological process: transmission of nerve impulse	0.0001	0.002	10/212
6	Cell adhesion: attractive and repulsive receptors	0.0001	0.002	9/175
7	Neurophysiological process: GABAergic neurotransmission	0.0008	0.013	7/138
8	Muscle contraction: relaxin signaling	0.002	0.029	30437
9	Reproduction: GnRH signaling pathway	0.002	0.029	7/166
10	Development: regulation of angiogenesis	0.003	0.035	8/223

G2 metabolic networks

1	Glutamic acid pathway	1×10^{-7}	8×10^{-6}	7/103
2	Glutamic acid pathways and transport	1×10^{-6}	4×10^{-5}	7/145
3	L-glutamate pathways and transport	9×10^{-6}	0.0003	6/131
4	L-ornithine pathways and transport	0.0001	0.002	5/124
5	Lyso-phosphatidylserine pathway	0.0003	0.005	4/81
6	Phosphatidylinositol-4,5-diphosphate pathway	0.005	0.08	3/92
7	Sphingomyelin pathway	0.006	0.08	3/97
8	Phosphatidylinositol-3,4,5-triphosphate pathway	0.03	0.3	2/66
9	[O-hexadecanoyl-(L)-carnitine pathway	0.03	0.31	2/71
10	1-hexadecanoyl-glycerol: 3-phosphate pathway	0.04	0.33	2/78

G2 GO processes

#	Process	p (uncorr)	p (FDR)	(Genes in data) (Genes total)
1	Synaptic transmission	7×10^{-15}	2×10^{-11}	33/856
2	Neuron differentiation	3×10^{-14}	5×10^{-11}	40/1346
3	Cell-cell signaling	1×10^{-13}	1×10^{-10}	38/1268
4	Generation of neurons	1×10^{-12}	7×10^{-10}	44/1795
5	Neuron development	2×10^{-12}	1×10^{-9}	34/1115
6	Nervous system development	5×10^{-12}	3×10^{-9}	54/2721
7	Neurogenesis	6×10^{-12}	3×10^{-9}	44/1891
8	Prepulse inhibition	8×10^{-12}	3×10^{-9}	41876
9	Regulation of synapse structure and activity	1×10^{-11}	5×10^{-9}	12/101
10	Startle response	2×10^{-11}	5×10^{-9}	15220

G3 pathway maps

#	Map	p (uncorr)	p (FDR)	(Genes in data) (Genes total)
1	Transcription: role of heterochromatin protein 1 (HP1) family in transcriptional silencing	5×10^{-6}	0.002	5/40
2	NF-AT signaling in cardiac hypertrophy	6×10^{-5}	0.01	5/65
3	Cell adhesion: ephrin signaling	0.0002	0.02	4/45
4	Signal transduction: IP3 signaling	0.0003	0.02	4/49
5	Immune response: mast cell proliferation, differentiation and survival	0.0009	0.06	3/30
6	Cell adhesion: gap junctions	0.0009	0.06	3/30
7	Development: angiopoietin - Tie2 signaling	0.001	0.07	3/35
8	Upregulation of MITF in melanoma	0.002	0.07	3/36
9	Transport: cAMP/Ca(2+)-dependent insulin secretion	0.003	0.1	3/43
10	Development: ligand-independent activation of ESR1 and ESR2	0.003	0.1	3/45

G3 process networks

#	Network	p (uncorr)	p (FDR)	(Genes in data) (Genes total)
1	Reproduction: gonadotropin regulation	1×10^{-5}	0.001	10/199
2	Reproduction: GnRH signaling pathway	0.0001	0.007	8/166
3	Cell adhesion: attractive and repulsive receptors	0.0002	0.007	8/175
4	Development: neurogenesis and axonal guidance	0.001	0.03	8/230
5	Cell cycle: G1-S growth factor regulation	0.002	0.05	7/195
6	Reproduction: progesterone signaling	0.01	0.27	6/214
7	Development: regulation of angiogenesis	0.02	0.28	6/223
8	Muscle contraction: nitric oxide signaling in the cardiovascular system	0.03	0.34	4/124
9	Translation: regulation of initiation	0.03	0.34	4/127
10	Transcription: chromatin modification	0.03	0.34	4/128

G3 metabolic networks

1	Phosphatidylinositol-3,4,5-triphosphate pathway	1×10^{-5}	0.001	5/66
2	1,2-dioleoyl-sn-glycerol: 3-phosphate pathway	6×10^{-5}	0.003	5/95
3	1,2-didocosahexaenoyl-sn-glycerol: 3-phosphate pathway	8×10^{-5}	0.003	5/99
4	Acyl-L-carnitine pathway	0.0007	0.02	4/89
5	Phosphatidylinositol pathway	0.004	0.09	2/21
6	Ceramide pathway	0.005	0.09	3/76
7	O-hexanoyl-(L)-carnitine pathway	0.007	0.1	3/86
8	Myristoyl-L-carnitine pathway	0.01	0.1	3/88

(*continued on next page*)

Table 1 (*continued*)

G3 pathway maps

#	Map	p (uncorr)	p (FDR)	(Genes in data) (Genes total)
9	1,2-didocosapentaenoyl-sn-glycerol: 3-phosphate pathway	0.01	0.1	3/91
10	Stearoylcarnitine pathway	0.01	0.11	3/97

G3 GO processes

#	Process	p (uncorr)	p (FDR)	(Genes in data) (Genes total)
1	Regulation of calcium ion transport into cytosol	9×10^{-13}	3×10^{-9}	13/107
2	Regulation of calcium ion transport	5×10^{-12}	8×10^{-9}	17/254
3	Regulation of localization	1×10^{-11}	2×10^{-8}	49/2455
4	Regulation of transport	3×10^{-10}	3×10^{-7}	40/1891
5	Regulation of epithelial cell migration	5×10^{-10}	4×10^{-7}	13/176
6	Regulation of metal ion transport	8×10^{-10}	5×10^{-7}	17/354
7	Transmembrane receptor protein tyrosine kinase signaling pathway	3×10^{-9}	1×10^{-6}	23/725
8	Negative regulation of release of sequestered calcium ion into cytosol	5×10^{-9}	2×10^{-6}	5/10
9	Blood vessel development	5×10^{-9}	2×10^{-6}	21/623
10	Regulation of release of sequestered calcium ion into cytosol	6×10^{-9}	2×10^{-6}	9/79

G4 pathway maps

#	Map	p (uncorr)	p (FDR)	(Genes in data) (Genes total)
1	Cell adhesion: ephrin signaling	4×10^{-5}	0.01	4/45
2	Neurophysiological process: EphB receptors in dendritic spine morphogenesis and synaptogenesis	0.0005	0.06	3/35
3	Transport: ACM3 in salivary glands	0.0008	0.07	3/42
4	Transport: alpha-2 adrenergic receptor regulation of ion channels	0.001	0.07	3/47
5	O-glycan biosynthesis	0.002	0.11	3/60
6	O-glycan biosynthesis/human version	0.0024	0.11	3/62
7	Amitraz-induced inhibition of insulin secretion	0.004	0.13	2/22
8	Development: delta- and kappa-type opioid receptors signaling via beta-arrestin	0.004	0.13	2/23
9	Neurophysiological process: dopamine D2 receptor transactivation of PDGFR in CNS	0.006	0.13	2/26
10	Neurophysiological process: GABA-B receptor signaling at postsynaptic sides of synapses	0.006	0.13	2/26

G4 process networks

#	Network	p (uncorr)	p (FDR)	(Genes in data) (Genes total)
1	Cytoskeleton: regulation of cytoskeleton rearrangement	0.0003	0.03	7/183
2	Cell adhesion: cell-matrix interactions	0.0007	0.03	7/211
3	Cell adhesion: attractive and repulsive receptors	0.001	0.05	6/175
4	Cell adhesion: synaptic contact	0.002	0.05	6/184
5	Cytoskeleton: actin filaments	0.008	0.16	5/176
6	Neurophysiological process: GABAergic neurotransmission	0.02	0.28	4/138
7	Development: regulation of angiogenesis	0.02	0.29	5/223
8	Development: neurogenesis and Axonal guidance	0.02	0.29	5/230
9	Reproduction: FSH-beta signaling pathway	0.03	0.3	4/160
10	Reproduction: GnRH signaling pathway	0.03	0.3	4/166

G4 metabolic networks

1	1,2-didocosahexaenoyl-sn-glycerol: 3-phosphate pathway	1×10^{-5}	0.0005	5/99
2	Phosphatidylinositol-3,4,5-triphosphate pathway	5×10^{-5}	0.001	4/66
3	1,2-dioleoyl-sn-glycerol: 3-phosphate pathway	0.0002	0.003	4/95
4	1,2-didocosapentaenoyl-sn-glycerol: 3-phosphate pathway	0.003	0.03	3/91
5	1-icosatrienoyl-sn-glycero-3-phosphocholine pathway	0.006	0.05	3/122
6	1-docosahexaenoyl-glycerol: 3-phosphocholine pathway	0.008	0.05	3/131
7	2-arachidonoyl-glycerol: 3-phosphocholine pathway	0.009	0.06	3/140
8	[O-hexadecanoyl-(L)-carnitine pathway	0.02	0.11	2/71
9	Acyl-L-carnitine pathway	0.03	0.12	2/89
10	Phosphatidylinositol-4,5-diphosphate pathway	0.03	0.12	2/92

G4 GO processes

#	Process	p (uncorr)	p (FDR)	(Genes in data) (Genes total)
1	Neuron development	5×10^{-8}	0.0001	24/1115
2	Neuron differentiation	4×10^{-7}	0.0004	25/1346
3	Neurogenesis	6×10^{-7}	0.0004	30/1891
4	Generation of neurons	7×10^{-7}	0.0004	29/1795
5	Synaptic transmission	9×10^{-7}	0.0004	19/856
6	Cell development	9×10^{-7}	0.0004	31/2031
7	Cell projection organization	1×10^{-6}	0.0004	23/1231
8	Dendritic spine development	2×10^{-6}	0.0007	4/16
9	Cell adhesion	3×10^{-6}	0.0007	20/1015
10	Thymus development	3×10^{-6}	0.0007	6/66

4.1. G1

This gene component was significantly correlated with the structural component S1 involving paralimbic cortical thickness (anterior cingulate, entorhinal and parahippocampal regions). GeneGO analysis showed this component to be associated with the Go Processes of synaptic transmission, nervous system development, and dendritic spine morphogenesis. The G1 component also included genes related to immune function (IL4, IL13), CLOCK function (NPAS2) (Soria et al., 2010) as well those involved in brain developmental processes such as cell adhesion and migration (EMCN, C9orf126, RCAN2 and CCDC80).

4.2. G2

Gene component 2 included several genes related to GABA function (GABBR2, GRM8) and showed significant associations with the S2 component comprised by frontoparietal thickness and subcortical volumes (thalamus, putamen and hippocampal). This is consistent with the implication of altered GABBR2 in schizophrenia (Fatemi et al., 2013). Glutamate related genes were also present in this network, including GRM8 polymorphisms that have previously been associated with schizophrenia (Takaki et al., 2004) and autism spectrum disorder (Li et al., 2008a, b). Pathway analysis revealed that pathways associated with G2 were related to voltage-gated channels or ion transport. Within those pathways and loading on the genetic component were CLSTN2, involved in calcium synthesis and linked to age-related episodic memory loss, (Pantzar et al., 2014; Sédille-Mostafaie et al., 2012) and with a potential role in cognitive symptoms in psychotic disorders. KCNQ5, a potassium voltage-gated channel gene, has been linked to schizophrenia (Kendler et al., 2011) and autism spectrum disorder (Gilling et al., 2013); and SLC22A5, a cation transporter gene, is involved in integrity of the blood brain barrier (Lucas et al., 2014) reported to be impaired in schizophrenia (Stolp et al., 2009).

Other pathways include neurogenesis (PROX1) (Yu et al., 2014), and neuronal signaling pathway, including the genes GNAI1, implicated in CREB signaling and long term depression; SYT2 (synaptotagmin2), a transmembrane protein which serves as a calcium sensor in the regulation of neurotransmitter release (Lucas et al., 2014); and zDHHC14 that is involved in S-acylation (also known as palmitoylation) which is critical for neuronal signaling. Other pathways associated with this genetic component included those involved in gluconeogenesis, (FBP2) and signaling (NKAIN2, which interacts with Na+, K+ ATPase). A strong association has been found between a gene in this cluster ADAMTS16 and physical functioning in schizophrenia (McGrath et al., 2013).

4.3. G3

Several genes in this gene cluster are involved in embryonic development, specifically neuronal migration and axon guidance (NXPH1), neuronal proliferation and migration (CHN2, SRGAP3, and DGK1). LAMB4 and NXPH1 are implicated in autism (Maestrini et al., 2010; Salyakina et al., 2011; Shen et al., 2010), CHN2 is implicated in GWAS studies of schizophrenia in males (Hashimoto et al., 2005), whereas DGK1 has been implicated in a GWAS study of SZ and bipolar disorder (Williams et al., 2010). The association of genes expressed in early brain development with cortical surface area but not volume is consistent with evidence that genetic influences underlying cortical surface area and thickness are independent and suggests that the former may be influenced by genes that are critical for early brain growth and development (Panizzon et al., 2009).

4.4. G4

This gene cluster was correlated with structural component (S3) comprising specific cortical surface areas. Cell adhesion, cytoskeleton structure, and phospholipid regulation were the enriched functional processes most associated with gene clusters in G4. RP1L1, involved in cell differentiation and implicated in autism (Glancy et al., 2009), was negatively correlated with this structural component. Regulation of cytoskeleton rearrangement, and cell adhesion (cell-matrix interactions, attractive and repulsive receptors, synaptic contact) pathways were, in fact, representative of genes throughout the G4 genetic component. Metabolic processes included the phosphatidic acid pathway; abnormal phospholipid distribution has been found in schizophrenia and those at familial risk for schizophrenia (Tandon N et al., 2013).

4.5. Implications

The structural-genetic networks identified here by parallel ICA comprise regional brain measures that have been reported as heritable biomarkers for psychotic disorders; our own observations of heritability ranges of 0.55–0.88 for these measures (Nanda et al., 2014) are consistent with this. A previous parallel ICA study of a small sample of schizophrenia patients showed genetic associations with a similar set of frontal and temporal brain regions (Jagannathan et al., 2010). Findings of involvement of specific brain structures (frontal, temporal, parietal, and subcortical) observed in previous structural imaging studies were replicated in our study. These regions have been evaluated as schizophrenia endophenotypes (Keshavan et al., 2007), and are herein partially validated. Previous investigators concluded that measures of both surface area and thickness were both highly heritable, but were essentially independent genetically (Hartberg et al., 2011; Panizzon et al., 2009). Our findings extend this notion by revealing somewhat distinct genetic pathways that are associated with each measure in a large sample of psychotic patients and healthy controls. They indicate that whatever the direct structural influences on these measures may be, upstream influences include developmental processes for surface area, and both immune response and intra-cellular signaling pathways for thickness.

Notably, the structural-genetic networks correlating with the subcortical volume and thickness components differ in their constituent pathways. The pathways for the SNPs in the genetic components associated with cortical surface areas and subcortical volume were related to three developmental processes that are critical for the expansion of cortical surface area: cell growth, neuronal migration, and cell differentiation. On the other hand, pathways for the SNPs loading onto the genetic components associated with thickness fall into three broad categories: glutamatergic function, synaptic function, and neuronal signaling. Interestingly, cortical thickness in paralimbic regions was associated with genes that mediate voltage-gated ion channels as well as those related to immune function. A growing body of literature implicates disturbances in ion channels as underlying not only SZ and bipolar disorder, but several other developmental and autoimmune neuropsychiatric disorders; ion channels and immune mechanisms may also offer promising therapeutic targets (Imbrici et al., 2013). Likewise, several lines of evidence including genetic association studies point to immune disturbances in SZ and other neuropsychiatric disorders, yet again pointing to potential novel therapeutic targets (Michel et al., 2012).

The strengths of this study rest on three key attributes; first, rather than only looking at one part of the psychosis spectrum e.g. bipolar disorder or schizophrenia, the entire psychosis spectrum was assessed simultaneously, acknowledging that there is likely similarity in the pathophysiological processes underlying these disorders with considerable clinical overlap. Second, the imaging data used for the parallel ICA were high-resolution images that underwent rigorous quality control testing and were processed using state of the art imaging software. Third, the parallel ICA method yielded clusters of SNPs both functionally related to each other and to cortical thickness, volume, or surface area. This clustering of SNPs into functionally related groups affords a degree of inference previously unavailable to the miscellany of univariate-

significant SNPs revealed in prior literature (Pearlson, Liu and Calhoun, 2015).

Limitations of our study include first, the relatively small sample size by the standards of genome-wide association studies, but the para-ICA method is well-suited to working with the sample size (n = 482) used. Second, we did not have genetic data from relatives of these probands. Third, even though we observed several known risk genes in this study, para-ICA revealed several others whose significance remains unclear. Finally, our sample included mostly medicated patients, and the effects of antipsychotics can bias our structural results.

Taken together, our observations provide a translational bridge between susceptibility genes, candidate pathophysiological processes known to be implicated in psychosis, and the observed brain structural alterations. They add to a growing body of evidence indicating the feasibility of utilizing structural brain abnormalities as endophenotypes across schizophrenia and other psychiatric disorders and precisely defining their genetic basis, thereby enabling a dissection of the complex disease mechanisms underlying psychotic disorders. Our findings generate testable hypotheses about the specific pathways from risk genes to aberrant neural circuits to disease expression. As our genomic and neuroscience technologies become increasingly powerful, their rigorous application and integrating information derived from them is essential to elucidating the hitherto mysterious etio-pathogenesis of psychotic disorders (Bigos and Weinberger, 2010; Thompson et al., 2014).

Supplementary data to this article can be found online at http://dx.doi.org/10.1016/j.schres.2016.10.026.

Conflict of interest

Dr. John Sweeney has received support from Takeda, Bristol-Meyers Squibb, Pfizer, Eli Lilly, Takeda, Roche and Janssen. Dr. Matcheri Keshavan has received support from Sunovion and GlaxoSmithKline. Dr. Carol Tamminga has received funding from Astellas, Eli Lilly, Cypress Biosciences, Merck, Sunovion, Intracellular Therapies, Lundback, and PureTech Ventures. Dr. Pearlson has served on an advisory panel for Bristol-Myers Squibb. Other authors declare no financial interest in relation to the work described in this manuscript other than the grant funding.

Funding

This study was supported by funding from National Institute of Mental Health through linked R01 MH077851 to Drs. Godfrey Pearlson, MH078113 to Carol Tamminga, MH077945 to Matcheri Keshavan, MH077862 to John Sweeney and MH077852 to Dr. Gunavant Thaker. Additional support includes 2R44 MH075481 to Dr. Gualberto Ruaño.

Contributors

MSK, GDP, CAT, JAS, and BAC designed the study and wrote the protocol. GR, AW, MK undertook data processing for the gene data. NT and ITM undertook data processing for imaging data. NT, JP, SME, BN, and SAM undertook data analysis. SEB and TLP collaborated on data analysis and interpretation. NT wrote the first draft of the manuscript. All authors contributed to and have approved the final manuscript.

Acknowledgements

We would like to thank all the research assistants and coordinators for the BSNIP study for their contributions to the data analyzed in this paper.

References

Anderson, C.A., Petterson, F.H., Clarke, G.M., Cardon, L.N., Morris, A.P., Zondervan, K.T., 2010. Data quality control in genetic case-control association studies. Nat. Protoc. 5, 1564–1573.

Arnold, S.J., Ivleva, E.I., Gopal, T.A., Reddy, A.P., Jeon-Slaughter, H., Sacco, C.B., Francis, A.N., Tandon, N., Bidesi, A.S., Witte, B., Poudyal, G., Pearlson, G.D., Sweeney, J.A., Clementz, B.A., Keshavan, M.S., Tamminga, C.A., 2015. Hippocampal volume is reduced in schizophrenia and schizoaffective disorder but not in psychotic bipolar I disorder demonstrated by both manual tracing and automated parcellation (FreeSurfer). Schizophr. Bull. 41 (1), 233–249.

Bigos, K.L., Weinberger, D.R., 2010. Imaging genetics - days of future past. NeuroImage 53, 804–809.

Calhoun, V.D., Adali, T., Pearlson, G.D., Pekar, J.J., 2001. A method for making group inferences from functional MRI data using independent component analysis. Hum. Brain Mapp. 14, 140–151.

Calhoun, V.D., Liu, J., Adali, T., 2009. A review of group ICA for fMRI data and ICA for joint inference of imaging, genetic, and ERP data. NeuroImage 45, S163–S172.

Chen, J., Calhoun, V.D., Pearlson, G.D., Ehrlich, S., Turner, J.A., Ho, B.C., Wassink, T.H., Michael, A.M., Liu, J., 2012. Multifaceted genomic risk for brain function in schizophrenia. NeuroImage 61, 866–875.

Dawy, Z., Sarkis, M., Hagenauer, J., Mueller, J., 2008. Fine-scale gene mapping using independent components analysis. IEEE/ACM Trans. Comput. Biol. Biotransform. 5, 448–460.

dbSNP, 1998. Database of Single Nucleotide Polymorphisms, Bethesda (MD): National Center for Biotechnology Information. National Library of Medicine (dbSNP Build ID: 142).

Desikan, R.S., Ségonne, F., Fischl, B., Quinn, B.T., Dickerson, B.C., Blacker, D., Buckner, R.L., Dale, A.M., Maguire, R.P., Hyman, B.T., Albert, M.S., Killiany, R.J., 2006. An automated labeling system for subdividing the human cerebral cortex on MRI scans into gyral based regions of interest. NeuroImage 31 (3), 968–980.

Ellison-Wright, I., Bullmore, E., 2010. Anatomy of bipolar disorder and schizophrenia: a meta-analysis. Schizophr. Res. 117, 1–12.

Endris, V., Wogatzky, B., Leimer, U., Bartsch, D., Zatyka, M., Latif, F., Maher, E.R., Tariverdian, G., Kirsch, S., Karch, D., Rappold, G.A., 2002. The novel Rho-GTPase activating gene MEGAP/srGAP3 has a putative role in severe mental retardation. Proc. Natl. Acad. Sci. U. S. A. 99 (18), 11754–11759.

Fatemi, S.H., Folsom, T.D., Rooney, R.J., Thuras, P.D., 2013. Expression of GABAA α2-, β1- and ε-receptors are altered significantly in the lateral cerebellum of subjects with schizophrenia, major depression, and bipolar disorder. Transl. Psychiatry 3, e303.

First, M.B., Spitzer, R.L., Gibbon, M., Williams, J.B.W., 2002. Structured Clinical Interview for DSM-IV-TR Axis 1 Disorders, Research Version, Patient Edition (SCID-I/P). Biometrics Research, New York State Psychiatric Institute, New York.

Gatt, J.M., Burton, K.L.O., Wiiliams, L.M., Schofield, P.R., 2015. Specific and common alleles implicated across major mental disorders: a review of meta-analysis studies. J. Psychiatr. Res. 60, 1–13.

Gilling, M., Rasmussen, H.B., Calloe, K., Sequeira, A.F., Baretto, M., Oliveira, G., Almeida, J., Lauritsen, M.B., Ullmann, R., Boonen, S.E., Brondum-Nielsen, K., Kalscheuer, V.M., Tümer, Z., Vicente, A.M., Schmitt, N., Tommerup, N., 2013. Dysfunction of the heteromeric kv7.3/kv7.5 potassium channel is associated with autism spectrum disorders. Front. Genet. 4, 54.

Glahn, D.C., Knowles, E.E., McKay, D.R., Sprooten, E., Raventós, H., Blangero, J., Gottesman, I.I., Almasy, L., 2014. Arguments for the sake of endophenotypes: examining common misperceptions about the use of endophenotypes in psychiatric genetics. Am. J. Med. Genet. B: Neuropsychiatr. Genet. 165, 122–130.

Glancy, M., Barnicoat, A., Vijeratnam, R., de Souza, S., Gilmore, J., Huang, S., Maloney, V.K., Thomas, N.S., Bunyan, D.J., Jackson, A., Barber, J.C., 2009. Transmitted duplication of 8p23.1-8p23.2 associated with speech delay, autism and learning difficulties. Eur. J. Hum. Genet. 17 (1), 37–43.

Gottesman, I.I., Gould, T.D., 2003. The endophenotype concept in psychiatry: etymology and strategic intentions. Am. J. Psychiatry 160, 636–645.

Gratten, J., Wray, N.R., Keller, M.C., Visscher, P.M., 2014. Large-scale genomics unveils the genetic architecture of psychiatric disorders. Nat. Neurosci. 17 (6), 782–790.

Hartberg, C.B., Sundet, K., Rimol, L.M., Haukvik, U.K., Lange, E.H., Nesvåg, R., Dale, A.M., Melle, I., Andreassen, O.A., Agartz, I., 2011. Brain cortical thickness and area correlates of neurocognitive performance in patients with schizophrenia, bipolar disorder, and healthy adults. J. Int. Neuropsychol. Soc. 17, 1080–1093.

Hashimoto, R., Yoshida, M., Kunugi, H., Ozaki, N., Yamanouchi, Y., Iwata, N., Suzuki, T., Kitajima, T., Tatsumi, M., Kamijima, K., 2005. A missense polymorphism (H204R) of a Rho GTPase-activating protein, the chimerin 2 gene, is associated with schizophrenia in men. Schizophr. Res. 73, 383–385.

Hill, S.K., Reilly, J.L., Keefe, R.S., Gold, J.M., Bishop, J.R., Gershon, E.S., Tamminga, C.A., Pearlson, G.D., Keshavan, M.S., Sweeney, J.A., 2013. Neuropsychological impairments in schizophrenia and psychotic bipolar disorder: findings from the bipolar-schizophrenia network on intermediate phenotypes (B-SNIP). Am. J. Psychiatry 170, 1275–1284.

Hyman, S.E., 2010. The diagnosis of mental disorders: the problem of reification. Annu. Rev. Clin. Psychol. 6, 155–179.

Imbrici, P., Camerino, D.C., Tricarico, D., 2013. Major channels involved in neuropsychiatric disorder and therapeutic perspectives. Front. Genet. 4, 76.

Insel, T.R., Cuthbert, B.N., 2009. Endophenotypes: bridging genomic complexity and disorder heterogeneity. Biol. Psychiatry 66, 988–989.

Ivleva, E.I., Bidesi, A.S., Keshavan, M.S., Pearlson, G.D., Meda, S.A., Dodig, D., Moates, A.F., Lu, H., Francis, A.N., Tandon, N., Schretlen, D.J., Sweeney, J.A., Clementz, B.A., Tamminga, C.A., 2013. Gray matter volume as an intermediate phenotype for psychosis: bipolar-schizophrenia network on intermediate phenotypes (B-SNIP). Am. J. Psychiatry 170, 1285–1296.

Jack Jr., C.R., Bernstein, M.A., Fox, N.C., Thompson, P., Alexander, G., Harvey, D., Borowski, B., Britson, P.J., L Whitwell, J., Ward, C., Dale, A.M., Felmlee, J.P., Gunter, J.L., Hill, D.L., Killiany, R., Schuff, N., Fox-Bosetti, S., Lin, C., Studholme, C., DeCarli, C.S., Krueger, G., Ward, H.A., Metzger, G.J., Scott, K.T., Mallozzi, R., Blezek, D., Levy, J., Debbins, J.P., Fleisher, A.S., Albert, M., Green, R., Bartzokis, G., Glover, G., Mugler, J., Weiner, M.W., 2008. The Alzheimer's disease neuroimaging initiative (ADNI): MRI methods. J. Magn. Reson. Imaging 27 (4), 685–691.

Jagannathan, K., Calhoun, V.D., Gelernter, J., Stevens, M.C., Liu, J., Bolognani, F., Windemuth, A., Ruaño, G., Assaf, M., Pearlson, G.D., 2010. Genetic associations of brain structural networks in schizophrenia: a preliminary study. Biol. Psychiatry 68 (7), 657–666.

Kapur, S., Phillips, A.G., Insel, T.R., 2012. Why it has taken so long for biological psychiatry to develop clinical tests and what to do about it? Mol. Psychiatry 17, 1174–1179.

Kendler, K.S., Kalsi, G., Holmans, P.A., Sanders, A.R., Aggen, S.H., Dick, D.M., Aliev, F., Shi, J., Levinson, D.F., Gejman, P.V., 2011. Genomewide association analysis of symptoms of

alcohol dependence in the molecular genetics of schizophrenia (MGS2) control sample. Alcohol. Clin. Exp. Res. 35 (5), 963–975.
Keshavan, M.S., Prasad, K.M., Pearlson, G., 2007. Are brain structural abnormalities useful as endophenotypes in schizophrenia? Int. Rev. Psychiatry 19, 397–406.
Keshavan, M.S., Tandon, R., Boutros, N.N., Nasrallah, H.A., 2008. Schizophrenia, "Just the Facts": what we know in 2008. Part 3: neurobiology. Schizophr. Res. 106, 89–107.
Keshavan, M.S., Morris, D.W., Sweeney, J.A., Pearlson, G., Thaker, G., Seidman, L.J., Eack, S.M., Tamminga, C., 2011a. A dimensional approach to the psychosis spectrum between bipolar disorder and schizophrenia: the schizo-bipolar scale. Schizophr. Res. 133, 250–254.
Keshavan, M.S., Tandon, R., Nasrallah, H.A., 2011b. Schizophrenia: just the "Facts". Part 6. From the elephant to the mouse. Schizophr. Res. 126, 3–14.
Kraepelin, E., 1919. Dementia Praecox and Paraphrenia. E & S Livingston, Edinburgh.
Li, H., Li, Y., Shao, J., Li, R., Qin, Y., Xie, C., Zhao, Z., 2008a. The association analysis of RELN and GRM8 genes with autistic spectrum disorder in Chinese Han population. Am. J. Med. Genet. B Neuropsychiatr. Genet. 147B (1), 194–200.
Li, M., Li, C., Guan, W., 2008b. Evaluation of coverage variation of SNP chips for genome-wide association studies. Eur. J. Hum. Genet. 16, 635–643.
Liu, J., Demirci, O., Calhoun, V.D., 2008. A parallel independent component analysis approach to investigate genomic influence on brain function. IEEE Signal Process Lett. 15, 413–416.
Lucas, E.K., Dougherty, S.E., McMeekin, L.J., Reid, C.S., Dobrunz, L.E., West, A.B., Hablitz, J.J., Cowell, R.M., 2014. PGC-1alpha provides a transcriptional framework for synchronous neurotransmitter release from parvalbumin-positive interneurons. J. Neurosci. 34, 14375–14387.
Maestrini, E., Pagnamenta, A.T., Lamb, J.A., Bacchelli, E., Sykes, N.H., Sousa, I., Toma, C., Barnby, G., Butler, H., Winchester, L., Scerri, T.S., Minopoli, F., Reichert, J., Cai, G., Buxbaum, J.D., Korvatska, O., Schellenberg, G.D., Dawson, G., de Bildt, A., Minderaa, R.B., Mulder, E.J., Morris, A.P., Bailey, A.J., Monaco, A.P., IMGSAC, 2010. High-density SNP association study and copy number variation analysis of the AUTS1 and AUTS5 loci implicate the IMMP2L-DOCK4 gene region in autism susceptibility. Mol. Psychiatry 15 (9), 954–968.
Mathworks, Natick, MA. www.mathworks.com, 2011.
McDonald, C., Marshall, N., Sham, P.C., Bullmore, E.T., Schulze, K., Chapple, B., Bramon, E., Filbey, F., Quraishi, S., Walshe, M., Murray, R.M., 2006. Regional brain morphometry in patients with schizophrenia or bipolar disorder and their unaffected relatives. Am. J. Psychiatry 163, 478–487.
McGrath, L.M., Cornelis, M.C., Lee, P.H., Robinson, E.B., Duncan, L.E., Barnett, J.H., Huang, J., Gerber, G., Sklar, P., Sullivan, P., Perlis, R.H., Smoller, J.W., 2013. Genetic predictors of risk and resilience in psychiatric disorders: a cross-disorder genome-wide association study of functional impairment in major depressive disorder, bipolar disorder, and schizophrenia. Am. J. Med. Genet. B Neuropsychiatr. Genet. 162B (8), 779–788.
Meda, S.A., Narayanan, B., Liu, J., Perrone-Bizzozero, N.I., Stevens, M.C., Calhoun, V.D., Glahn, D.C., Shen, L., Risacher, S.L., Saykin, A.J., Pearlson, G.D., 2012. A large scale multivariate parallel ICA method reveals novel imaging-genetics relationships for Alzheimer's disease in the ADNI cohort. NeuroImage 60, 1608–1621.
Meda, S.A., Ruaño, G., Windemuth, A., O'Neil, K., Berwise, C., Dunn, S.M., Boccaccio, L.E., Narayanan, B., Kocherla, M., Sprooten, E., Keshavan, M.S., Tamminga, C.A., Sweeney, J.A., Clementz, B.A., Calhoun, V.D., Pearlson, G.D., 2014. Multivariate analysis reveals genetic associations of the resting default mode network in psychotic bipolar disorder and schizophrenia. Proc. Natl. Acad. Sci. U. S. A. 111 (19), E2066–E2075.
Michel, M., Schmidt, M.J., Mirnics, K., 2012. Immune system dysregulation in autism and schizophrenia. Dev. Neurobiol. 72 (10), 1277–1287.
Nanda, P., Tandon, N., Mathew, I.T., Giakoumatos, C.I., Abhishekh, H.A., Clementz, B.A., Pearlson, G.D., Sweeney, J., Tamminga, C.A., Keshavan, M.S., 2014. Local gyrification index in probands with psychotic disorders and their first-degree relatives. Biol. Psychiatry 76 (6), 447–455.
Palaniyappan, L., Balain, V., Liddle, P.F., 2012. The neuroanatomy of psychotic diathesis: a meta-analytic review. J. Psychiatr. Res. 46, 1249–1256.
Panizzon, M.S., Fennema-Notestine, C., Eyler, L.T., Jernigan, T.L., Prom-Wormley, E., Neale, M., Jacobson, K., Lyons, M.J., Grant, M.D., Franz, C.E., Xian, H., Tsuang, M., Fischl, B., Seidman, L., Dale, A., Kremen, W.S., 2009. Distinct genetic influences on cortical surface area and cortical thickness. Cereb. Cortex 19, 2728–2735.
Pantzar, A., Laukka, E.J., Atti, A.R., Papenberg, G., Keller, L., Graff, C., Fratiglioni, L., Bäckman, L., 2014. Interactive effects of KIBRA and CLSTN2 polymorphisms on episodic memory in old-age depression. Neuropsychologia 62, 137–142.
Pearlson, G.D., Liu, J., Calhoun, V.D., 2015. An introductory review of parallel independent component analysis (p-ICA) and a guide to applying p-ICA to genetic data and imaging phenotypes to identify disease-associated biological pathways and systems in common complex disorders. Front. Genet. 6, 276.
Price, A.L., Patterson, N.J., Plenge, R.M., Weinblatt, M.E., Shadick, N.A., Reich, D., 2006. Principal components analysis corrects for stratification in genome-wide association studies. Nat. Genet. 38, 904–909.
Purcell, S., Neale, B., Todd-Brown, K., Thomas, L., Ferreira, M.A., Bender, D., Maller, J., Sklar, P., de Bakker, P.I., Daly, M.J., Sham, P.C., 2007. PLINK: a tool for whole-genome association and population-based linkage analyses. Am. J. Hum. Genet. 81, 559–575.
Rachakonda, S., Liu, J., Calhoun, V., 2008. Fusion ICA toolbox (FIT) manual. The MIND Research Network, University of New Mexico, Albuquerque, NM.
Salyakina, D., Cukier, H.N., Lee, J.M., Sacharow, S., Nations, L.D., Ma, D., Jaworski, J.M., Konidari, I., Whitehead, P.L., Wright, H.H., Abramson, R.K., Williams, S.M., Menon, R., Haines, J.L., Gilbert, J.R., Cuccaro, M.L., Pericak-Vance, M.A., 2011. Copy number variants in extended autism spectrum families reveal candidates potentially involved in autism risk. PLoS One 6 (10), e26049.
Sédille-Mostafaie, N., Sebesta, C., Huber, K.R., Zehetmayer, S., Jungwirth, S., Tragl, K.H., Fischer, P., Krugluger, W., 2012. The role of memory-related gene polymorphisms, KIBRA and CLSTN2, on replicate memory assessment in the elderly. J. Neural Transm. 119 (1), 77–80.
Shen, L., Kim, S., Risacher, S.L., Nho, K., Swaminathan, S., West, J.D., Foroud, T., Pankratz, N., Moore, J.H., Sloan, C.D., Huentelman, M.J., Craig, D.W., Dechairo, B.M., Potkin, S.G., Jack Jr., C.R., Weiner, M.W., Saykin, A.J., 2010. Alzheimer's disease neuroimaging initiative. Whole genome association study of brain-wide imaging phenotypes for identifying quantitative trait loci in MCI and AD: a study of the ADNI cohort. Neuroimage 53 (3), 1051–1063.
Soria, V., Martínez-Amorós, E., Escaramís, G., Valero, J., Pérez-Egea, R., García, C., Gutiérrez-Zotes, A., Puigdemont, D., Bayés, M., Crespo, J.M., Martorell, L., Vilella, E., Labad, A., Vallejo, J., Pérez, V., Menchón, J.M., Estivill, X., Gratacòs, M., Urretavizcaya, M., 2010. Differential association of circadian genes with mood disorders: CRY1 and NPAS2 are associated with unipolar major depression and CLOCK and VIP with bipolar disorder. Neuropsychopharmacology 35 (6), 1279–1289.
Stolp, H.B., Dziegielewska, K.M., 2009. Review: role of developmental inflammation and blood-brain barrier dysfunction in neurodevelopmental and neurodegenerative diseases. Neuropathol. Appl. Neurobiol. 35 (2), 132–146.
Sui, J., Pearlson, G., Caprihan, A., Adali, T., Kiehl, K.A., Liu, J., Yamamoto, J., Calhoun, V.D., 2011. Discriminating schizophrenia and bipolar disorder by fusing FMRI and DTI in a multimodal CCA + joint ICA model. NeuroImage 57, 839–855.
Takaki, H., Kikuta, R., Shibata, H., Ninomiya, H., Tashiro, N., Fukumaki, Y., 2004. Positive associations of polymorphisms in the metabotropic glutamate receptor type 8 gene (GRM8) with schizophrenia. Am. J. Med. Genet. B Neuropsychiatr. Genet. 125B (1), 6–14.
Tamminga, C.A., Ivleva, E.I., Keshavan, M.S., Pearlson, G.D., Clementz, B.A., Witte, B., Morris, D.W., Bishop, J., Thaker, G.K., Sweeney, J.A., 2013. Clinical phenotypes of psychosis in the bipolar-schizophrenia network on intermediate phenotypes (B-SNIP). Am. J. Psychiatry 170, 1263–1274.
Tandon, R., Keshavan, M.S., Nasrallah, H.A., 2008. Schizophrenia, "Just the Facts" 2. Epidemiology and etiology. Schizophr. Res. 102, 1–23.
Tandon, N., Bolo, N.R., Sanghavi, K., Mathew, I.T., Francis, A.N., Stanley, J.A., Keshavan, M.S., 2013. Brain metabolite alterations in young adults at familial high risk for schizophrenia using proton magnetic resonance spectroscopy. Schizophr. Res. 148 (1–3), 59–66.
Thompson, P.M., Stein, J.L., Medland, S.E., et al., 2014. The ENIGMA Consortium: large-scale collaborative analyses of neuroimaging and genetic data. Brain Imaging Behav. http://dx.doi.org/10.1007/s11682-013-9269-5.
Williams, S.R., Aldred, M.A., Der Kaloustian, V.M., Halal, F., Gowans, G., McLeod, D.R., Zondag, S., Toriello, H.V., Magenis, R.E., Elsea, S.H., 2010. Haploinsufficiency of HDAC4 causes brachydactyly mental retardation syndrome, with brachydactyly type E, developmental delays, and behavioral problems. Am. J. Hum. Genet. 87 (2), 219–228.
Yu, D.X., Di Giorgio, F.P., Yao, J., Marchetto, M.C., Brennand, K., Wright, R., Mei, A., McHenry, L., Lisuk, D., Grasmick, J.M., Silberman, P., Silberman, G., Jappelli, R., Gage, F.H., 2014. Modeling hippocampal neurogenesis using human pluripotent stem cells. Stem Cell Rep. 3 (1), 217.